Gas Phase Chemistry in Cellulose Fast Pyrolysis

ARTICLE *in* INDUSTRIAL & ENGINEERING CHEMISTRY RESEARCH · DECEMBER 2009

Impact Factor: 2.59 · DOI: 10.1021/ie801280g

3 AUTHORS, INCLUDING:

Roberto Lanza
KTH Royal Institute of Technology
14 PUBLICATIONS **147** CITATIONS
SEE PROFILE

Paolo Canu
University of Padova
93 PUBLICATIONS **1,124** CITATIONS
SEE PROFILE

Gas Phase Chemistry in Cellulose Fast Pyrolysis

R. Lanza, D. Dalle Nogare, and P. Canu*

Università di Padova, Dipartimento di Principi e Impianti di Ingegneria Chimica, Via Marzolo 9, 35131 Padova, Italy

We experimentally and theoretically studied cellulose pyrolysis at high temperature and short residence time. We investigated the gas phase chemistry with dedicated experiments and feeding intermediates. Results have been also compared with equilibrium calculations, both single (gas) phase and allowing for solid C formation. Our aim was to understand the cellulose degradation mechanism and particularly the role of gas phase chemistry. We provided evidence of a simplified mechanism, where CO formation is a first, fast step that can be related to levoglucosan ring opening, while H_2 comes from a totally different route, based on hydrocarbon reforming reactions, which also provide further CO. In addition, butadiene was identified as a key intermediate in the decomposition sequence. The different paths and rates of CO formation and H_2 formation explain why the ratio of CO to H_2 is not constant, particularly at short residence time. A two-stage process or longer contact time is required, if aiming at syngas production.

1. Introduction

It has been confirmed that biomass pyrolysis is a viable route for producing gases and liquids that can replace some petroleum-derived products. The possibility of obtaining useful chemicals has also been demonstrated.[1] The interest in these technologies is based on the widespread availability of a renewable source of energy that does not contribute to increasing atmospheric CO_2 levels. Although pyrolysis is meant to be applied to raw biomass, laboratory experiments must concentrate on a more chemically defined material, to limit the variability of the results. It is commonly agreed that cellulose can be a model species for biomass because it is the most frequent and sometimes the most abundant biomass component. Such an assumption is not fully satisfactory, both because cellulose is only partially representative of biomass and because cellulose itself is not a precisely defined chemical species, given that its properties depend on the polymerization degree and the production process. In any case, because of the complexity of biomass pyrolysis, data obtained on cellulose represent a good starting point.

Several fast pyrolysis techniques have been suggested,[2] some of which have been developed to a commercial scale. Reference 3 provides a thorough review of the pyrolysis processes involving rapid heating and low residence times, now recognized as fast pyrolysis, and the status of their applicability. Many researchers agree that variations in the contact time and the temperature can lead to completely different products. This fact clearly indicates the existence of a not elementary mechanism for the overall process, including mass- and energy-transport steps. To understand how selectivity is influenced by process conditions, some laboratory experiments in which these variables are carefully controlled and hopefully single processes are isolated are required. At the least, physical and chemical processes must be distinguished to be quantified independently. Note that the combination of temperature level and contact time is frequently addressed in the literature in terms of the heating rate (HR), somewhat drawing attention away from the prime variables.

In our view, the features of the entrained-flow reactor (EFR) are unique with respect to the investigation of fast processes with interactions between chemical and physical processes, and its difficulties can be overcome by means of suitable modeling of the results.[4] It is worth emphasizing that a flow reactor can, in principle, overcome the limitations of the dynamics of both the heating system (heating coils, heating grids, Curie point supports, radiant lamps) and the measuring technique (temperature and composition). These features appear to have been clearly exploited in two papers,[5,6] where a significant effort was devoted to the in-depth characterization of the reactor and the reacting cellulose so that a kinetically controlled pyrolysis could be obtained. The conclusion of these studies was that a laminar EFR is a useful tool for generating unique and significant data on the high-temperature behavior of reacting solids. These authors extensively used CFD modeling to design and characterize their EFR and compared their findings with literature kinetics results. In contrast, we report modeling characterization and kinetics speculation, independently of literature values, in a companion paper.[7] The EFR reactor is only one of the multiple choices for fast pyrolysis:[8] the use of so many diverse techniques demonstrates how difficult the investigation of the pyrolysis of solids at high temperatures and short residence times is.

There are a lot of studies about the pyrolysis of biomass at low temperature and slow heating rates, but only a few concerning the fast pyrolysis that seems to be a valid process to convert inferior quality stuff in fuels or chemicals. For this reason we interested ourselves in the study of the reaction at high temperatures and low residence times and concentrated our attention both in the gas composition and in the decomposition mechanisms.

2. Experimental Apparatus

Data have been collected in a flow reactor, where cellulose is fed as a powder, entrained by an inert gaseous carrier. We call such a configuration an entrained-flow reactor (EFR). A schematic picture of it is shown in Figure 1.

The EFR is a 5 mm i.d. quartz tube, inside three independent heating sections, each one approximately 0.4 m long and delivering a maximum of 500 W. Temperatures above 900 °C can be easily reached and stably maintained. At the outlet of the quartz tube quenching of the products is provided. The cold trap is set at −20 °C, in an NaCl/water bath kept in a Dewar, stable at this temperature for at least 3 h. The trap outlet is connected to a gas chromatographic (GC) analyzer. We used

* To whom correspondence should be addressed.

10.1021/ie801280g CCC: $40.75
Published on Web 12/19/2008

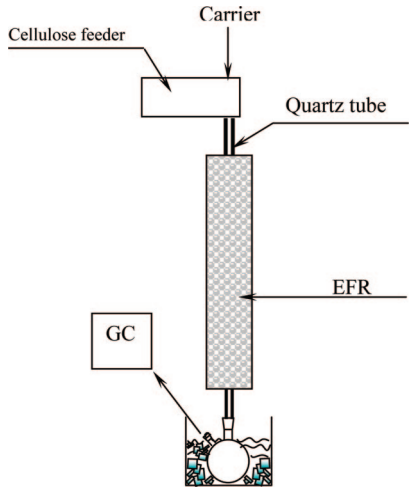

Figure 1. Schematic representation of the EFR.

Table 1. Particle Size Distribution by Weight in the Five Classes Considered and Its Variation with Passage through the Screw Feeder

size range (μm)	wt %, after screening	σ/ mean (%)	wt %, after screw feeder	σ/ mean (%)
38−44	12.4	−0.8	12.6	0.8
64−74	8.95	0.2	8.94	0.1
101−112	8.76	−0.2	8.70	−0.9
150−160	8.27	0.2	8.25	0.0
201−212	4.60	−0.4	4.61	−0.2

an HP 6890, with a Porapak Q column and TCD/FID in series. For the analyses of the products obtained in some homogeneous phase tests, a Varian microGC 4900 equipped with a Poraplot U and 5 Å molecular sieve, has been used. The cellulose powder is fed through a micro screw feeder. It allows extremely low and stable mass flow rates in the 0.03−0.5 g/min range. Before entering the reactor, cellulose is mixed with the carrier gas in a small tube that runs across the screw feeder. Product quantification and identification is obtained by gravimetric determinations (weight difference of each part of the apparatus) and online gas analysis and offline characterization of the residue.

The cellulose was Avicel PH 102 from FMC Europe S.A. The original material was first classified in 15 size intervals. We concentrated on five of these, for further tests in the reactor. Classification was quite a tedious task, because of the nature of the material (weight, shape, and surface properties) and the number of classes used, down to 38 μm. In addition, we feared that the rather long screening time (approaching 3 h) and the following manipulation in the screw feeder could modify the particle size distribution (PSD), because of mechanical stresses on the particles. The PSD in the five classes considered is reported in Table 1, both after classification and after passage through the screw feeder.

Note that these classes amounted to approximately 43% of the total mass of Avicel and each one of the 15 classes had a weight percent around 4−10%, notwithstanding the nominal size of 90 μm given by the supplier. Table 1 allows concluding that the material withstands quite relevant stresses without significant dimensional modifications. However, scanning electron microscopic (SEM) images, shown in Figure 2, clearly indicate that only the larger size is approximately spherical and reasonably monodispersed. In addition, the porosity that determines the hygroscopic behavior is quite evident. Accordingly, the material was always dried right before feeding it to the reactor, to guarantee reproducible experiments and results. For this purpose,

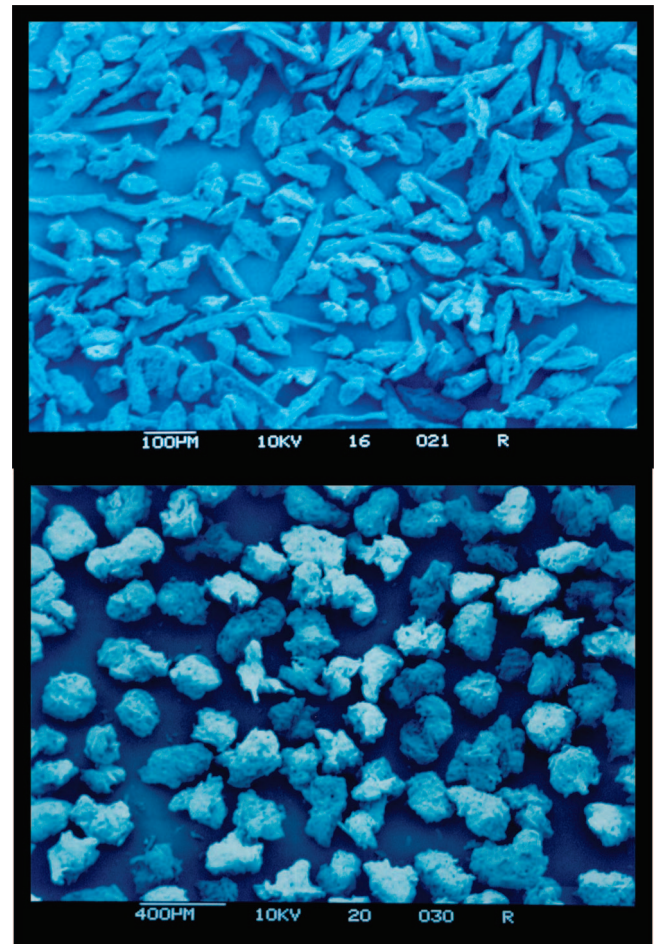

Figure 2. SEM images of cellulose Avicel PH 102 in two size classes: 38−44 μm (above) and 201−212 μm (below).

we kept the cellulose in an oven, at 105 °C; after approximately 1 h the weight stabilized, indicating that all the adsorbed water was removed. Because of the low oven temperature, we assumed that there were no chemical or morphological modifications in the powder.

3. Experimental Observations

We investigated the role of reaction temperature and actual residence time in the reactor on the product distribution, in terms of both macroproducts (gas, tar, and char) and individual gases. Other variables were not changed, after a thorough investigation to identify the best operating conditions. Such variables include the particle size, the solid humidity, and the gas to solid ratio in the feed. According to the results of a previous study,[12] which have been checked again after some structural modifications to the reactor, the feed was always a diluted suspension of cellulose, in a single size range, and preliminarily dried. Flow rates were 0.04−0.06 g/min cellulose and 1 L/min helium at 20 °C as carrier gas. As already observed,[12] under these conditions the suspension is diluted enough to prevent particle−particle interactions and then solids concentration effects. We ran a series of preliminary tests to determine the influence of the particle size on the results at 900 °C, and we concluded that the five classes of Table 1 do not result in any significant difference. This is also confirmed by Funazukuri.[11] We then performed all the following investigations only with the larger size (200−212 μm), because of its more regular shape, also better suited to subsequent modeling. The negligible effect of particle size might appear in contrast with previous observa-

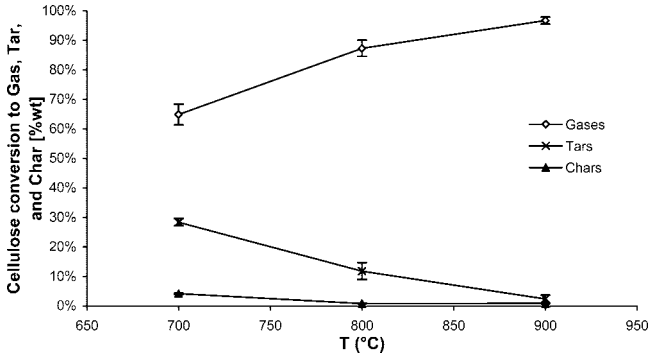

Figure 3. Macroproduct distribution at different temperatures, in terms of mass fraction of the cellulose fed. Complete cellulose conversion is always achieved at these temperatures.

Table 2. Average Gas Temperature above 350 °C in the Reactor, with 1 L/min Helium and Varying the Number of Heating Elements (HE) in Series

	set temperature (°C)		
no. of HE	700	800	900
1	611	513	538
2	650	731	795
3	650	731	824

tions,[12] where results for Avicel PH 102 and PH 200 were compared. According to the supplier, Avicel PH 102 and Avicel PH 200 have nominal average sizes of $d_p = 90$ μm and $d_p = 180$ μm, respectively. Previous observations indicated a lower cellulose conversion at 500 °C with the larger size, supposed to be 180 μm, vs 90 μm. Results of the present investigation allow concluding that (1) the original material is very broadly distributed, so that the nominal size can be poorly informative, and meaningful tests require further classification, as done here and (2) the original material contains a nonnegligible amount of particles quite larger than the average diameter, much more vulnerable to transport resistances.

3.1. Effect of Temperature. The influence of the temperature on the reaction products was studied in the 700−900 °C range. Lower temperatures were previously investigated[12] and resulted in fairly limited cellulose conversion (<60% at 600 °C, < 30% at 500 °C), making the investigation of the gas composition rather questionable. As already reported,[9−11] above 700 °C the cellulose conversion can be complete. Among products, the gas yield varies significantly, being less than 65 wt % at 700 °C and almost complete at 900 °C. This is consistent with a previous work,[9] where 98% conversion of cellulose to gaseous products at 900 °C has been obtained. The measured gas, tar, and char yields are shown in Figure 3 as a function of the oven set temperature, which is the prevailing (and maximum) temperature reached by the gas flowing through. Because of flow and oven geometry, the species are not exposed to this temperature for the whole reactor length. An average gas temperature perceived by traveling cellulose can be determined from the experimental, axial temperature profiles. We conventionally assumed that relevant temperatures are those exceeding 350 °C and then weighted the local temperature with local residence time (eq 1), obtaining a time-averaged temperature:

$$\bar{T} = \int_{z_1}^{z_2} \frac{T(z)}{v(z)}\,\mathrm{d}z = \int_0^{\theta} \frac{T(t)}{v(t)}\,\mathrm{d}t \qquad (1)$$

where z_1 and z_2 are the axial positions and $T(z)$ is above the conventional threshold of 350 °C. Note that the same calculation yields a conventional residence time, discussed later. Table 2 summarizes the averaged gas temperatures using a different number of heating elements.

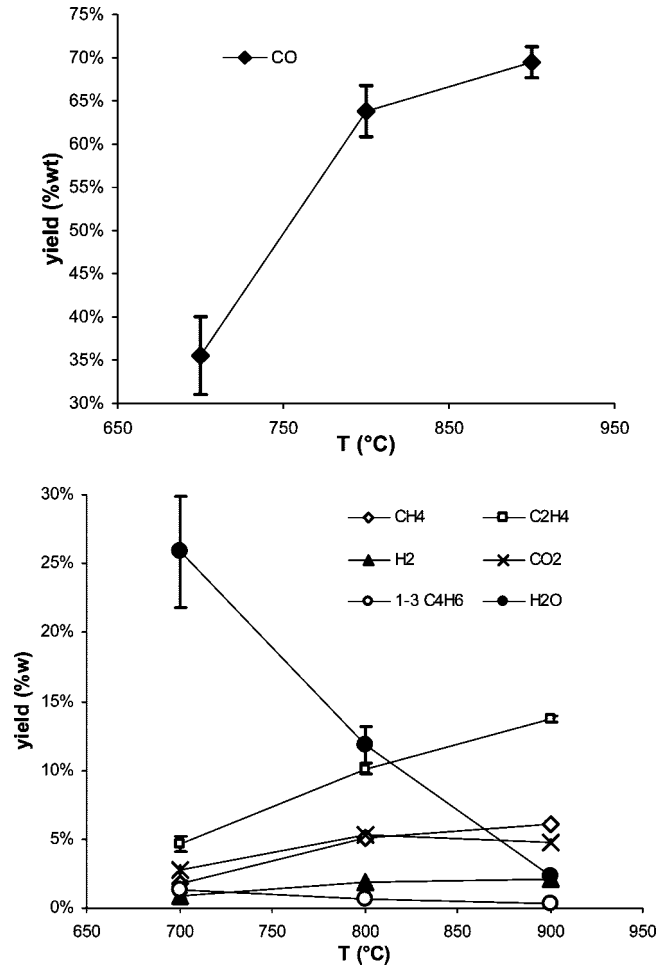

Figure 4. CO, H_2, CO_2, H_2O, and light hydrocarbon yields by weight (mass flow rate of each gas by cellulose mass feeding rate), as a function of temperature.

Product distributions for all cases in Table 2 are reported in Figure 3, together with the corresponding experimental uncertainties ($\pm\sigma$) determined with two or three replicated measurements.

Distinction between gas and tar is based on the cold trap temperature, from which gases exit at a temperature always between −8 and −15 °C; the trap is in a very stable bath at −20 °C. Accordingly, "tar" can contain water as well, as discussed below. Yields are calculated as the weight ratio between the single products and the cellulose powder fed; mass flow rates are used for the purpose. Figure 3 clearly indicates that gases are always the main product above 700 °C. At 900 °C the cellulose conversion into gas is almost complete. Char yield at these temperatures is always very low, and tar yield is appreciable below approximately 800 °C, but becomes negligible at the higher temperature.

Figure 4 shows how the yield of the main gaseous products is affected by the temperature. CO is the most abundant gas, and its yield increases dramatically from 700 to 800 °C, approaching an asymptote as the temperature rises further. Note that CO_2 is also present in an appreciable amount, but it apparently stabilizes with temperature and slightly decreases above 800 °C. Ethane, propane, and propylene have been also measured, but at very low concentration (yields always less than 0.1 wt %). H_2, CH_4, and C_2H_4 show a steady increase with temperature. C_2H_2 is also likely to be present, but GC analysis with Porapak Q cannot separate C_2H_2 and C_2H_4, resulting in cumulated data. Results compare well with previous results by

Graham et al.[9] and by Scott et al.,[10] confirming the consistency of the experimental investigation.

We tried to go further into the interpretation of the mechanism and specifically the role of homogeneous, secondary reactions, discussed later. For that purpose, we concentrated our attention on C_4's, H_2, and H_2O. Other peaks in the chromatograms are due to C_4's, but at very low concentration; the most abundant (thus quantifiable) was identified as 1,3-C_4H_6 and is included in Figure 4. However, 1,3-butadiene reaches at most 1.3 wt % of cellulose fed, too small for any industrial application, but it is extremely important to speculate about the degradation mechanism. 1-C_4H_8 was also identified, but its concentration was very low, and quantification was questionable. The reproducible measurements of C_4's in our Avicel degradation tests do not imply that thermal degradation of raw cellulose (or even worse, biomass) can yield the same product, due to their heterogeneous nature and the relevance of impurities in affecting the chemistry.

We determined the water content in the condensed matter that we defined as "tar" by Karl Fischer analysis. Unexpectedly, most of the "tar" content obtained at high temperature was just water, varying from 97 to 100% of the total mass condensed, above 800 °C. This is not actually so surprising considering that cellulose has a high content of water in its structure (that can be considered as $[C_6(H_2O)_5]_n$). Nonetheless, also including this water in the results shown in Figure 4, we see that water yield decreases when the temperature rises, implying that it gets involved in some reaction at high temperature.

Interpretation of data in Figure 4 must take into account that all the species increase their yields partially as a consequence of the overall increase of gas yields shown in Figure 3. In addition, the large difference of molar mass between H_2 and the other species underestimates its relevance when compared on a mass basis. However, on a molar basis, the H_2 yield is larger than that of many of the other species.

3.2. Effects of Residence Time. The experimental apparatus was designed to allow variations of the residence time in the high-temperature region. Two options are available for this purpose, i.e., variations of either the carrier gas flow rate or the number of heating elements, or both. In this study we varied the heating length only, because the carrier flow rate can affect the quality and stability of the gas−solid suspension, introducing secondary, confusing effects on the conversion and gas yields. Consequently, the investigated range (between 250 and 400 ms) is quite limited. All the measurements have been taken at 900 °C because of the highest yield of gas achievable. The residence time has been calculated from the axial temperature profile, $T(z)$, assuming that the carrier behaves as an ideal gas, which expands and contracts instantaneously as the temperature varies along its path. Consequently, mass conservation yields the local velocity, $v(z) = v_{IN}T(z)/T_{IN}$, which can be used to calculate the progressive residence time, $\theta(z)$:

$$\theta(z) = \int_{z_1}^{z} \frac{dz}{v(z)} \tag{2}$$

When $z = z_2$, we obtain the residence time in the reactor portion where $T > 350$ °C, used to compare our results.

Surprisingly, the residence time variations within this range do not significantly affect the results. The distribution of the products among gas, tar, and char remains approximately constant at 89, 10, and 1 wt %, respectively. Longer residence time causes a limited decrease (few percent) of gas, with a slight increase in the tar and mostly in the char yield. More appreciable effects can be observed on single gaseous products, as summarized in Figure 5. Lighter gases increase their amount from 250 to 295 ms and then stabilize, while heavier gases decrease with longer residence times, as expected.

Such behavior is consistent with a chain-cracking sequence that progressively reduces the molecular weight of the products. The cellulose polymeric molecules decompose to heavy hydrocarbons that successively crack into smaller and smaller ones, up to CO and H_2. Whether these species are the ultimate products, in case the temperature rises enough and sufficient reaction time is given, is not that obvious, as discussed later in comparing equilibrium calculations. Note, however, that most of the transformation is expected to occur in the gas phase, among gaseous species, as already suggested by Scott et al.[10] In order to understand the mechanism, we experimentally studied the homogeneous reactions between gas species in the *same* reactor, at comparable temperatures and flow rate. In addition, we investigated the thermodynamics of the observed gas species in the temperature range investigated.

3.3. Gas Phase Chemistry. Experimental evidence and physical intuition suggest that several crucial transformations leading to the final gas composition take place in the homogeneous gas phase.

An exploratory test was made feeding CO, H_2O, C_2H_4, and H_2 in the same reactor, at comparable conditions (particularly of temperature and residence time); these gases above 700 °C originated small quantities of CH_4 and C_2H_6, suggesting that radical reactions take place indeed. At 900 °C ethylene in the feed was substituted with iso-C_4H_8, which was one of the C_4's produced by the pyrolysis. Isobutene reacted much more than ethylene, and considerable amounts of CH_4, C_2H_4, C_2H_6, C_3H_6, and C_2H_8 were produced, consuming H_2, CO, and H_2O. Not surprisingly, these gas yields were comparable with those of the cellulose pyrolysis. Even the unreacted quantity of iso-C_4H_8 was similar to its amount in the cellulose pyrolysis. We can easily argue that C_4's are intermediates: they form from cellulose, but before leaving the reactor they may have enough time to convert to lighter species. In confirmation of this we see that the yield of C_4's in cellulose pyrolysis decreases with the temperature and also with the residence time (Figures 4 and 5).

To further analyze and understand the reactions occurring in the gas phase and the decomposition mechanism, we ran some tests feeding C_4's, water, and/or CO to the same reactor. In the first test (mix 1) we fed 3% of H_2O and 2.2% of 1-C_4H_8, varying the temperature between 600 and 900 °C. Results are shown in Figure 6.

At 600 °C no reaction takes place at this residence time. H_2O does not enter the chemistry over most of the temperature range, while clearly butene reacts, decomposing to lighter hydrocarbons (methane, ethylene, acetylene, and propylene) and also forming H_2. Very small amounts (<0.007%) of CO_2 and CO (not shown in Figure 6) are detected. When the temperature reaches 800 °C, butene is totally consumed and the further increase of lighter species (methane, ethylene, and acetylene) is sustained by propylene consumption. This further confirms that the light hydrocarbons come from the decomposition of heavier species, in sequential cascade of reaction with increasing activation energy.

An interesting observation during this test is the formation of appreciable amounts of tar (collected in the quench section), and indeed, as the temperature increases the mass balances on the gaseous products show a lack of matter. These facts indicate that the gas fed can also polymerize, forming heavier compounds. This is confirmed by a qualitative GC−MS analysis of tars, which evidenced the production of polyaromatic hydro-

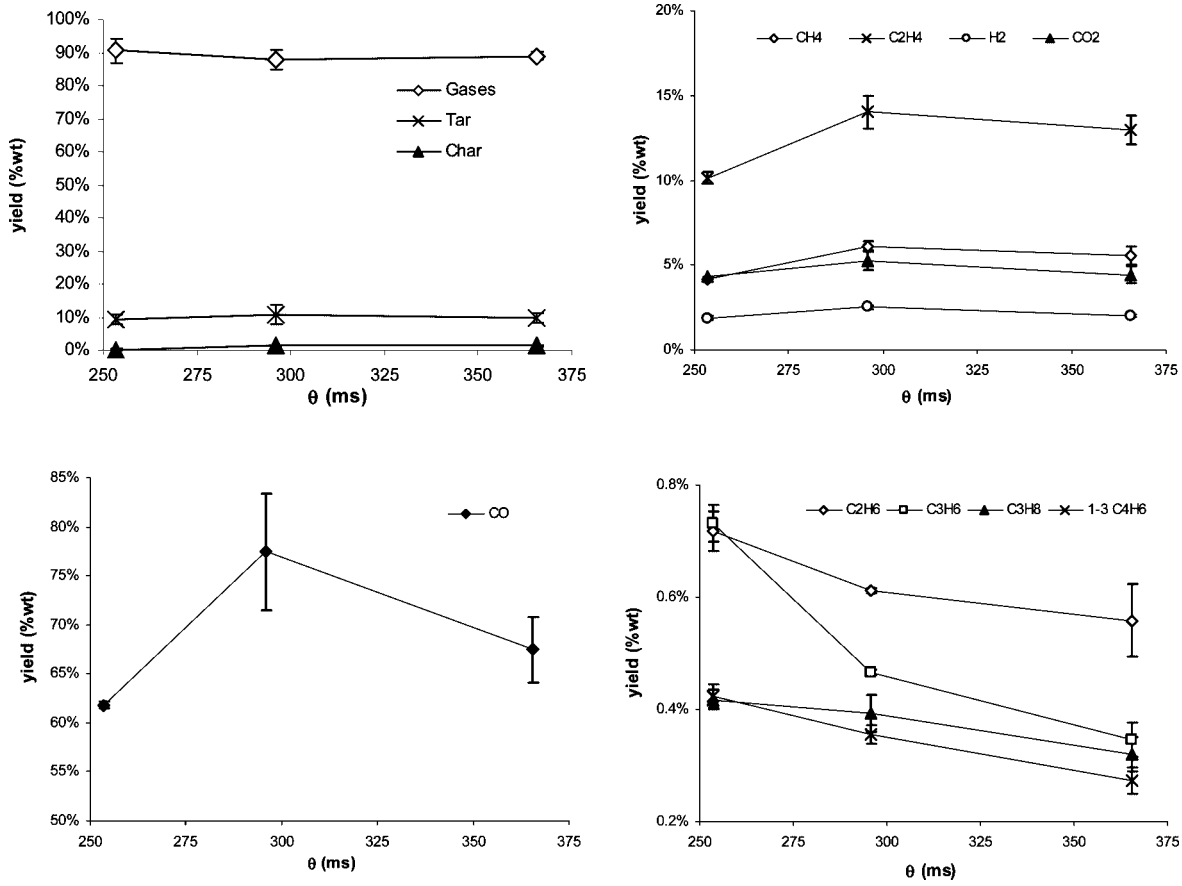

Figure 5. Massive yields of gaseous products as a function of residence time.

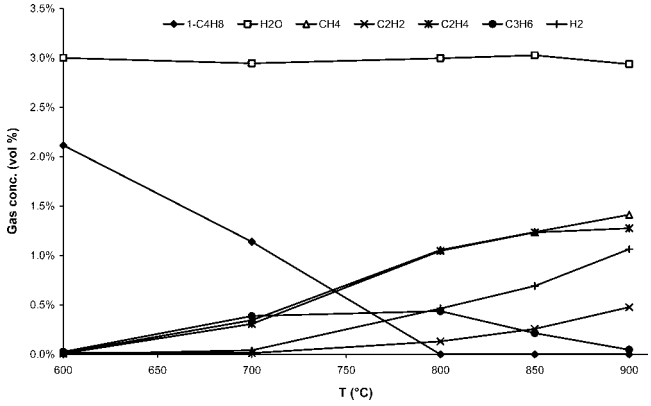

Figure 6. Gas composition at reactor exit as a function of temperature, detected feeding water, and 1-butene.

carbons (PAHs) and other compounds such as phenol, propionic acid, and methyl acetate with significant amounts of naphthalene and traces of a large number of other aromatic compounds. It is well-known and documented[1,13,14] that tars form in biomass and cellulose pyrolysis, but they are usually assumed to come from rearrangement of longer chains of heavier species and not from reactions between fairly simple molecules in the gas phase. This test proves, instead, that at least part of the tar formed during the pyrolysis is due to homogeneous reactions occurring in the gas phase.

Since butadiene was identified and quantified among the pyrolysis products, we ran some tests feeding it to the same reactor and θ, with steam and with or without CO; Figure 7 shows the results of these further experiments.

Again, H_2O does not react, no reactions are observed below 700 °C, and butadiene reacts to form lighter hydrocarbons. Comparing tests with and without CO, we see that its presence does not affect the product composition at all. Indeed, CO does not react when fed, but it is formed (in very small amounts) when H_2O is also in the feed. Besides that, H_2O is not significantly involved in any reaction, even varying its concentration in the different tests (3.8 and 2.8%, respectively).

In both tests with butadiene, with and without CO, the product distribution at different temperatures is similar to the test where 1-butene was fed. A few differences can be detected: first, 1,3-C_4H_6 does not react completely even at the highest temperatures reached; second, only traces of propylene are detected. Considering the different structure of the two C_4's, it is easy to understand that propylene formation is favored starting from 1-butene, just breaking the single bond between the C3 and C4 carbons, while the presence of two double bonds in the butadiene structure hinders the propylene formation. Another difference between the tests with butane and butadiene is the lower amount of H_2 (about half) produced from butadiene, and this is due to the lower amount of H available in its molecular structure, besides the lower C_4 conversion. The residual amount of 1,3-C_4H_6 and 1-C_4H_8 detected in these tests is consistent with the results of the pyrolysis test, where some butadiene is quantified, but only traces of butene are detected. Cellulose pyrolysis tests do not allow discerning if the butene production was very low or if it was produced in considerable amounts, but consumed right after, forming other gases, although at larger residence time its concentration decreases. Experiments feeding butene suggests that it reacts as soon as formed, turning mainly into C_3H_6 that further reacts as the temperature rises.

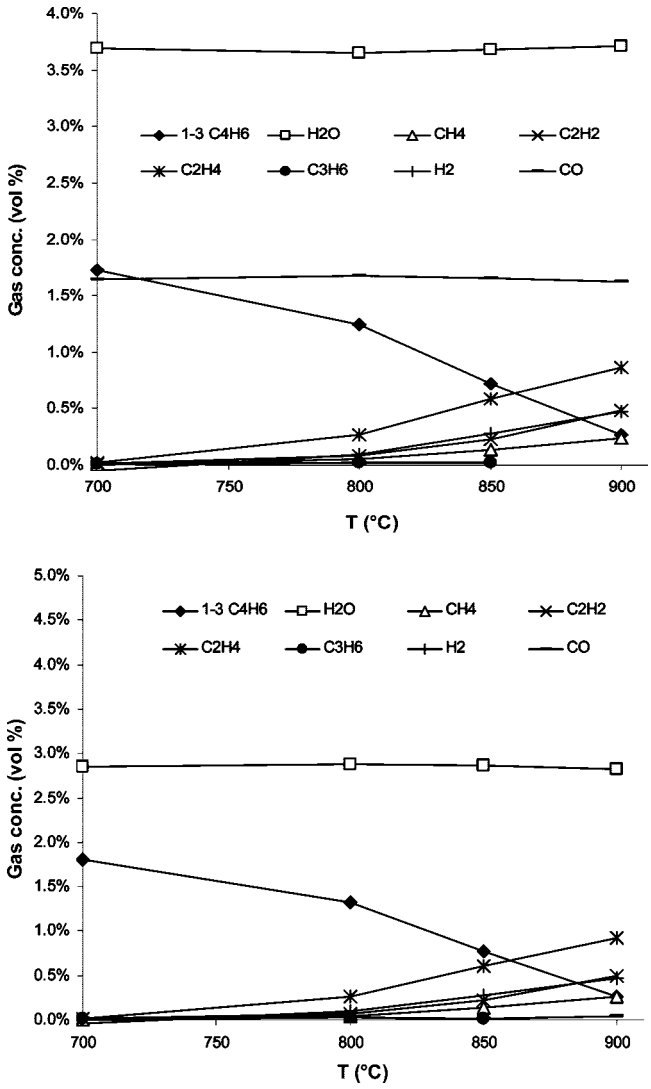

Figure 7. Gas composition detected feeding: 1,3-C_4H_6, H_2O, and CO (above, mix 2) and 1,3-C_4H_6 and H_2O (below, mix 3).

Besides the differences detected, feeding butadiene leads to the formation of a considerable amount of tar. Differently from the case of butene, GC−MS reveals that the residual contains only aromatic compounds, mostly consisting of biphenyl, naphthalene, fluorene, 1-methylnaphthalene, and phenanthrene, very similar to the analysis of the residual obtained from cellulose pyrolysis. This is quite an interesting observation, implying that the formation of 1,3-butadiene is favored on the formation of 1-C_4H_8 during the cellulose decomposition.

This series of homogeneous phase tests, along with the fact that C_4 species concentration decreases as contact time and temperature increase, confirm that cellulose decomposes forming progressively shorter hydrocarbons chains, further reacting to the final, light products (CO, H_2, CH_4, C_2H_4, C_2H_2, and H_2O), and butadiene is the most abundant intermediate.

The original evidence provided by homogeneous reaction carried out in the same reactor complements a picture quite well shaped by previous work.[1] Indeed, Piskorz et al.,[1] using very similar conditions (same Avicel PH 102 cellulose and temperature range, but much shorter residence time), proved that the cellulose chain breaks, giving shorter oligomers such as G_6+ down to cellotriosan, cellobiosan, and levoglucosan. The amount of the shorter oligomers increases with the residence time, confirming that they progressively form from heavier species.

Among all bonds of cellulose (see Figure 8), the glycosidic bond linking two glucose units is the weakest and then most likely to be thermally broken first, explaining the yield of short oligomers. Lighter cyclic compounds are obtained from glucopyranose, reacting to levoglucosan with H_2O production (Figure 9).

This is likely the main reaction that produces water, which is one of the primary products considering that the starting point is a cellulose (Avicel PH 102) with a rather small average degree of polymerization (DP) of about 200. Interestingly, Both Broido[15] and Shafizadeh[16] mechanisms describe the formation of a species called *active cellulose*, before the formation of char, tar, and gases. This active cellulose was found to have a DP of 200, against an initial value in excess of 2500; thus the first step of their mechanisms is a depolymerization that leads to the species we used as starting material in our experiments.

Levoglucosan is detected by a many authors as a cellulose pyrolysis product, and once formed, its bicyclic structure can open, breaking the bond between C1 and C2. This forms radicals (Figure 10) that can rapidly react, forming a wide range of compounds.

Once the ring has been opened, the other ring containing two oxygen atoms is likely to lead to the formation of CO (mainly), CO_2 (in small amounts as detected from the experimental tests), and short linear chains, e.g., C_4 if two CO molecules are formed and C_5 when a CO_2 molecule is produced. The formation of radicals brings a wide range of decomposing reactions (including radical rearrangements), leading to the production of lighter linear compounds. After these species are formed, the hydrocarbon chains further react, decomposing to lighter compounds as evidenced by the gas phase tests described in this work. Water can be further produced from $H^{\cdot}$ and $OH^{\cdot}$ radicals lost from the chain. However, gas phase experiments then proved that not all the H contained in the hydrocarbons can react further to molecular hydrogen.

4. Thermodynamic Calculations

The equilibrium composition of the decomposition products of cellulose has been calculated with the purpose of comparing it with experimental measurements and speculating on the pyrolysis mechanism. We used direct minimization of the total free energy as a function of mole distribution among a large set of species, under the constraints of atomic mass conservation. We carried out the calculation through Cantera,[17] with a multiphase approach to account for solid carbon (char) formation, and adopting the full NASA thermodynamic database. We calculated and isothermal, isobaric equilibrium, so the energetic issues are not relevant, avoiding speculating on the enthalpy of formation of the cellulose. The feedstock composition is 0.05 g/min cellulose in 1 L/min He at 20 °C. Cellulose was modeled assuming the atomic ratio C/H/O of 6/10/5, which is the only relevant input data. The resulting mass fraction of each atom in the feedstock is reported in Table 3.

The equilibrium predicts the presence of appreciable amounts only of C(s), CH_4, CO, CO_2, H_2, and H_2O, besides He. The solid phase (pure carbon) is very significant, an issue frequently overlooked by single (gas) phase equilibrium calculations. The gas phase is composed mainly of CO and H_2, in the same quantity, while CH_4, CO_2, and H_2O are 1 order of magnitude smaller.

A carbon-based species selectivity, defined as

$$S_i = \frac{\mathrm{mol}_i}{\sum \mathrm{mol}_i}, \quad i = \mathrm{C(s)}, \mathrm{CH_4}, \mathrm{CO}, \mathrm{CO_2} \tag{3}$$

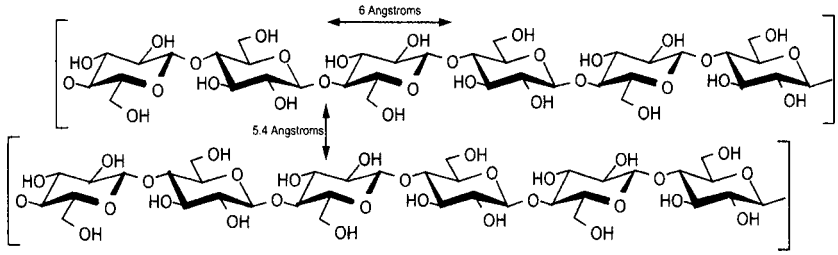

Figure 8. Cellulose structure with intermolecular distances.

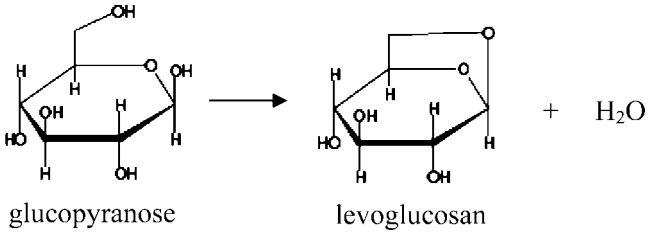

Figure 9. Formation of levoglucosan starting from glucopyranose.

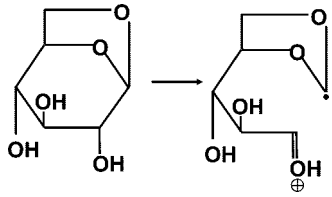

Figure 10. Levoglucosan ring opening leading to radical species.

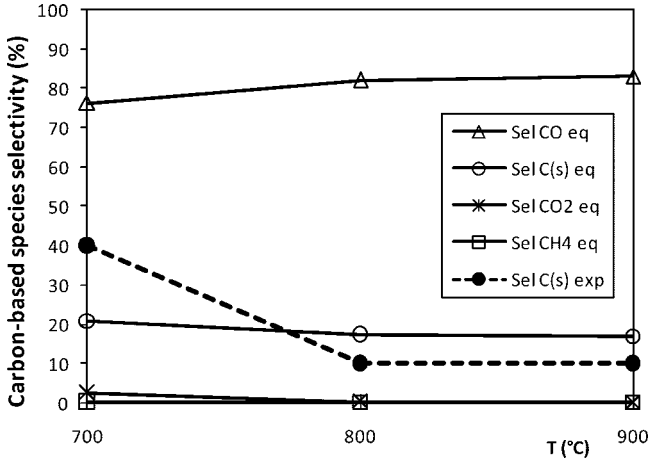

Figure 11. Selectivity of species containing carbon atoms, according to the multiphase equilibrium. Comparison with experimental selectivity to char.

Table 3. Atomic Composition, as Mass Fractions, of the Whole Feedstock and of the Gas Phase at Deprived by a Given Amount of Carbon

	feedstock (wt %)	gas (−10% C) (wt %)	gas (−40% C) (wt %)
He	0.769	0.777	0.802
C	0.103	0.094	0.064
O	0.114	0.115	0.119
H	0.014	0.014	0.015

can help in understanding the distribution of the products among the phases; see Figure 11. S_i is about 80% for CO and 20% for C(s), while CH_4 and CO_2 collect a marginal part of the available carbon. In the same figure, experimental char selectivity is compared with the equilibrium predictions. At 700 °C the measured char represents 40% of the total carbon fed to the system, while at 800 and 900 °C it reduces to 10%.

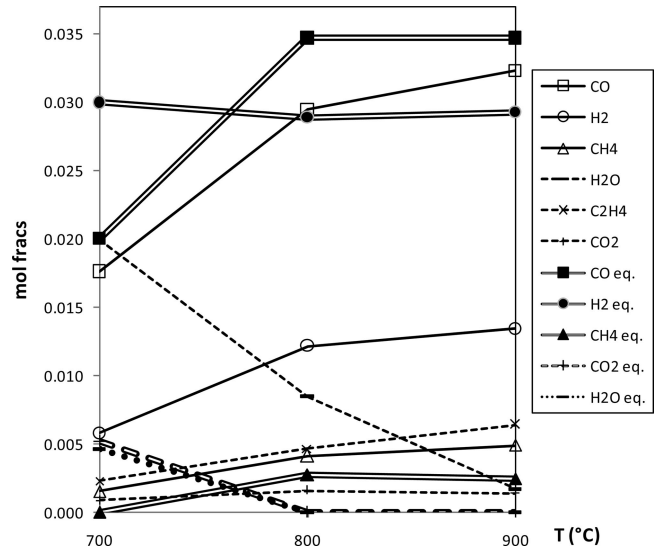

Figure 12. Molar fractions in the gas phase. Restricted equilibrium calculation. Experiment (single line) vs predictions (double line).

At higher temperature the equilibrium calculations predict almost twice the amount of solid carbon effectively measured. Consequently, the predicted composition of the gas phase is expected to be quite different from that from measurements, due to the lack of carbon available to form gas species containing it. We can conclude that solid phase formation is thermodynamically expected but in practice the short residence time of our experiments may limit its formation.

To attempt a comparison of the measured gas phase composition with equilibrium, a restricted form of equilibrium calculation was formulated. We calculated a single-phase equilibrium of a mixture that has the H and O amount of the feedstock, but the amount of C is reduced by 40% in one case (at 700 °C) or 10% in the others (at the higher temperatures). The modified gas mass fractions are reported in Table 3.

In Figure 12 the restricted, gas phase equilibrium predictions are compared with the experimental mole fractions. The CO equilibrium composition is slightly larger than in the experimental measurements, with the same trend. The value at 700 °C is lower, with the gas being short in C, while CO rises where the char selectivity drops to 10%. The CO equilibrium amount is the same for 800 and 900 °C, while the experimental one keeps increasing with the temperature, meaning that the decomposition reactions are faster at higher temperature. The last observation is a first hint that the actual reaction does not reach the equilibrium, but it tends toward it. The difference between the calculated and the measured amounts of H_2 is much larger than for CO. We believe this is a further confirmation of the mechanism formulated above, based on levoglucosan ring opening. According to that theory, CO forms in the early stages

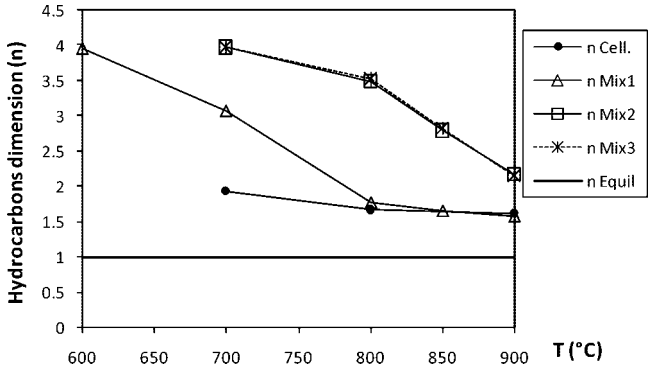

Figure 13. Mean dimension of hydrocarbons in the gas products, for cellulose pyrolysis, homogeneous experiments, and equilibrium calculations.

of the decomposition while H_2 requires the decomposition of the hydrocarbons and the reforming reactions to occur. Particularly, the steam reforming reactions that turn H_2O and CH_4 into CO and H_2 are known to have high activation energies, requiring higher temperatures to get to completion in such short contact times. As a confirmation, we measured more CH_4 and H_2O than predicted by the equilibrium, as well as lower CO and H_2 (Figure 12). Also, CO_2 is expected to react with CH_4 in the dry reforming reactions, for which the same observations valid for steam reforming apply.

The small variation in gas yield with residence time confirms that there are two chemical regimes: a faster one, correlated to the early stages of the cellulose breakage, and then a slower one, where high activation energy reactions occur. In light of the latter conclusion, the slower part of the pyrolysis may take advantage of a suitable catalyst, but also of addition of O_2 or H_2O to reduce the char formation and increase the syngas yield.

An interesting feature in the experimental data is the presence of ethylene, C_2H_4, not predicted by the equilibrium. Apparently, the levoglucosan chain breaks into water and hydrocarbons such as 1-butene, 1,3-butadiene, propane, propylene, ethane, ethylene, and methane, all of which were found in the experiments, but many were present only as traces while ethylene and methane have relevant molar fractions. As a matter of fact, the measured C_2H_4 was more than CH_4, confirming the existence of a progressive reduction of the dimension of the hydrocarbons, up to the equilibrium species, i.e., CH_4, CO, and H_2.

The progressive breakage of the hydrocarbon chains is further confirmed by the evaluation of their mean size, $\bar{n}$, defined as the number of carbon atoms in the molecule (eq 4).

$$\bar{n} = \frac{\sum n_i(\mathrm{mol}_i)}{\sum \mathrm{mol}_i}, \quad i = \mathrm{CH_4}, \mathrm{C_2H_4}, \mathrm{C_2H_6}, \mathrm{C_3H_6}, \mathrm{C_3H_8}, \text{1-}\mathrm{C_4H_6}, \text{1,3-}\mathrm{C_4H_8} \quad (4)$$

This is reported in Figure 13 for both experiments and equilibrium calculations. According to the equilibrium, only CH_4 is expected among the products ($\bar{n} = 1$), while in the experimental measurements $\bar{n}$ varies between 1.9 at 700 °C and 1.6 at 900 °C. In the same figure, $\bar{n}$ for the homogeneous experiments is reported. Starting from 1-butene, the inner composition varies already after 600 °C and reaches the values of the cellulose pyrolysis at about 800 °C. When 1,3-butadiene is fed, thanks to resonance the reactant mixture is stable up to 700 °C, after which it breaks more slowly than in the 1-butene case. Noticeably, the presence of CO or H_2O does not influence the cracking reactions, which occur at the same pace for mix 2 and mix 3. In all cases, molecules become lighter as temperature increases, because the fragmentation reactions get faster. Here again the approach of the equilibrium is clear, but limited by a residence time that is too short.

Equilibrium calculations (not shown) for the homogeneous experiments are quite dissimilar from the experimental measurments, where CO is hardly detectable and H_2 remains below 1%. The low presence of C_4's means that cracking reactions take place easily, unless in resonance stabilized molecules, which is confirmed by the residence time experiments, where their composition in the system is fairly constant and the olefin/paraffin ratios are rather high. The small amounts of CO and H_2 measured, when only hydrocarbons are fed, again confirm that some slow reforming reactions still have to go to completion, in the absence of a suitable catalyst.

5. Conclusions

With our experiments we explored aspects of cellulose fast pyrolysis that were apparently underestimated, aiming at better elucidating the decomposition mechanism. We first verified the effect of temperature and residence time over the reaction, with these variables being the most influential on the pyrolysis. We focused on the gaseous products, operating at high temperatures with high heating rates, at short residence times. We found that the temperature rise at short residence time increases the gas yield until almost 100% at 900 °C, confirming earlier observations. The main products are CO and H_2 on a volumetric basis, but also CH_4 and hydrocarbons up to four carbon atoms are measured, severely limiting the H_2 yield. Residence time does not influence significantly the gas product distribution, but may affect the char yield. The relative amount of larger molecules in the gas, such as C_3 and C_4, decreases with longer residence times. A catalyst able to turn hydrocarbons to CO and H_2, just operating in the gas phase, might improve the H_2/CO ratio. Otherwise, a further reduction of residence time is likely to allow significant production of unsaturated C_4's such as butene or butadiene, which are useful chemicals for synthesis.

Experiments dedicated to investigating the gas phase chemistry concluded that C_4's can effectively be significant intermediates in cellulose decomposition, but before leaving the reactor they may have enough time to convert to lighter species. Differently, CO and H_2O are unable to affect the chemistry (without a suitable catalyst), even at high temperature. Also tar formation from C_4's has been observed, supporting the hypothesis that it can be a side reaction through the whole decomposition sequence. Tar analysis also supports the evidence that butadiene is more likely as intermediate than butene.

From all the evidence we formulated the following simplified decomposition sequence:

$$\mathrm{cellulose} \rightarrow \mathrm{G}_m, \mathrm{H_2O}$$

$$\mathrm{G}_m, \mathrm{H_2O} \rightarrow \mathrm{C}_n, \mathrm{CO}, \mathrm{H_2O}\ (+\mathrm{CO_2}, \mathrm{H_2}), \quad \text{with } n \leq 4$$

$$\mathrm{C_4}, \mathrm{CO}, \mathrm{H_2O}\ (+\mathrm{CO_2}, \mathrm{H_2}) \rightarrow \mathrm{CH_4}, \mathrm{CO}, \mathrm{H_2O}\ (+\mathrm{CO_2}, \mathrm{H_2})$$

$$\mathrm{CH_4}, \mathrm{CO}, \mathrm{H_2O}\ (+\mathrm{CO_2}, \mathrm{H_2}) \rightarrow \mathrm{CH_4}, \mathrm{CO}, \mathrm{H_2}$$

Cellulose decomposes primarily to short oligomers (G_m) down to levoglucosan, which easily breaks to form mainly CO, H_2O, and higher (up to four C-atoms) hydrocarbons. The C_4's undergo thermal cracking reactions leading to CH_4. Reforming reactions finally lead to the equilibrium composition, i.e., syngas and residual CH_4. At the given temperatures and residence times, the route to syngas cannot go to completion; then H_2 yield is in

fact limited where different hydrocarbons such as CH_4, C_2's, and C_3's remain.

Thermodynamic equilibrium calculations, both multiphase and restricted to one phase, further confirm the picture. Although equilibrium is only approached at such short residence times, the closer the higher the temperature, it is clear that reforming reactions do not progress significantly in the uncatalyzed experiments. In addition, the formation of solid carbon severely affects also the CO yield, whose experimental measurements can be nicely approximated (in excess) only by a restricted equilibrium calculation, based on the only C available in the gas phase. This confirms that CO comes from a fast reaction (levoglucosan ring opening). On the other hand, the restricted equilibrium predicts much higher CH_4 and H_2 amounts than measured, further confirming that H_2 production is limited by the high activation energy of homogeneous reforming reactions.

We can conclude that the potential of cellulose (biomass) pyrolysis to be a viable source of syngas would benefit from a two-step reactor: a short contact time, high-temperature pyrolysis to gain the light hydrocarbon stage while minimizing char formation, and then a catalytic stage to bring the reforming to completion, possibly with water addition to increase syngas yield and reduce char.

Literature Cited

(1) Piskorz, J.; Majerski, P.; Radlein, D.; Vladars-Usas, A.; Scott, D. Flash Pyrolysis of Cellulose for Production of Anhydro-Oligomers. *J. Anal. Appl. Pyrolysis* **2000**, *56*, 145.

(2) Bridgwater, A.; Boocock, D. *Development in Thermochemical Biomass Conversion*; Blackie Academic and Professional: London, 1997.

(3) Bridgwater, A.; Peacocke, G. Fast Pyrolysis Processes for Biomass. *Renewable Sustainable Energy Rev.* **2000**, *4*, 1.

(4) Antal, M.; Varhegyi, G.; Jakab, E. Cellulose Pyrolysis Kinetics: Revisited. *Ind. Eng. Chem. Res.* **1998**, *37*, 1867.

(5) Brown, A.; Dayton, D.; Nimlos, M.; Daily, J. Design and Characterization of an Entrained Flow Reactor for the Study of Biomass Pyrolysis Chemistry at High Heating Rates. *Energy Fuels* **2001**, *15*, 1276.

(6) Brown, A.; Dayton, D.; Daily, J. A Study of Cellulose Fast Pyrolysis Chemistry and Global Kinetics at High Heating Rates. *Energy Fuels* **2001**, *15*, 1286.

(7) Rizzardi Soravia, D.; Canu, P. Kinetics Modeling of Cellulose Fast Pyrolysis in a Flow Reactor. *Ind. Eng. Chem. Res.* **2002**, *41*, 5990.

(8) Meier, D.; Faix, O. State of the art of Applied Fast Pyrolysis of Lignocellulosic Materials—a Review. *Bioresour. Technol.* **1999**, *68*, 71.

(9) Graham, R.; Mok, L.; Bergougnou, M.; De Lasa, H.; Freel, B. Fast pyrolysis (ultrapyrolysis) of cellulose. *J. Anal. Appl. Pyrolysis* **1984**, *6*, 363.

(10) Scott, D. S.; Piskorz, J.; Bergougnou, M. A.; Graham, R.; Overend, R. P. The Role of Temperature in the Fast Pyrolysis of Cellulose and Wood. *Ind. Eng. Chem. Res.* **1998**, *27*, 8.

(11) Funazukuri, T.; Hudgins, R.; Silveston, P. Product Distribution in Pyrolysis of Cellulose in a Microfluidized Bed. *J. Anal. Appl. Pyrolysis* **1986**, *9*, 139.

(12) Visentin, V.; Piva, F.; Canu, P. Experimental Study of Cellulose Fast Pyrolysis in a Flow Reactor. *Ind. Eng. Chem. Res.* **2002**, *41*, 4965.

(13) Sanders, E. B.; Goldsmith, A. I.; Jeffrey, I. Seeman A model that distinguishes the pyrolysis of D-glucose, D-fructose, and sucrose from that of cellulose. Application to the understanding of cigarette smoke formation. *J. Anal. Appl. Pyrolysis* **2003**, *66*, 29.

(14) Sjöström, K.; Chen, G.; Yu, Q.; Brage, C.; Rosén, C. Promoted reactivity of char in co-gasification of biomass and coal: synergies in the thermochemical process. *Fuel* **1999**, *78*, 1189.

(15) Broido, A.; Weinstein M. *Proceedings of the 3rd International Conference on Thermal Analysis*; Wiedemann, Ed.; Birkhauser Verlag: Basel, 1971; p 285.

(16) Bradbury, A. G. W.; Sakai, Y.; Shafizadeh, F. A Kinetic Model for Pyrolysis of Cellulose. *J. Appl. Polym. Sci.* **1979**, *23*, 3271.

(17) Goodwin, D. G. An open-source, extensible software suite for CVD process simulation. In *Proceedings of CVD XVI and EuroCVD Fourteen*; Allendorf, M., Teyssandier , F., Eds.; Electrochemical Society: Pennington, NJ, 2003; p 155.

Received for review August 22, 2008
Revised manuscript received November 12, 2008
Accepted November 13, 2008

IE801280G